Preparation and characterization of biodiesel waste-derived biomass for the removal of dye from contaminated water

Alagarasan Jagadeesh Kumar, Eldon R. Rene, Rajendra Prasad Singh, Shasikala Siddharthy, Jimin Xie, Chinnaiya Namasivayam and Yuanguo Xu

ABSTRACT

Lignocellulosic biodiesel waste of Jatropha husk (JH) was used to develop $ZnCl_2$ activated Jatropha husk carbon (ZAJHC). ZAJHC was applied as an adsorbent for the removal of methylene blue (MB) from contaminated water. Batch mode of adsorption experiments were carried out and the parameters investigated included agitation time, MB concentration (100–180 mg L^{-1}) and adsorbent dose (25–200 mg/50 mL). The adsorption of MB reached equilibrium at 120 min for 100 mg L^{-1}, 140 min for 120 mg L^{-1} and 160 min for other concentrations tested. Based on the Langmuir isotherm, the monolayer adsorption capacity (Q_0) was found to be 500 mg g^{-1}. The kinetic data were also fitted to the pseudo first-order, second-order and intraparticle diffusion models, and the experimental data followed closely the pseudo first-order kinetic model. Thermodynamic parameters such as standard enthalpy (ΔH° 3.86 J mol^{-1} K^{-1}), standard entropy (ΔS° 65.86 J mol^{-1} K^{-1}) and standard free energy (ΔG°) indicated the spontaneous nature of MB adsorption by ZAJHC. The adsorption was found to be endothermic in nature. Alkaline pH was favourable for the adsorption of MB. The pH effect and desorption studies suggest that ion-exchange might be the possible mechanism governing the adsorption process.

Key words | adsorption kinetics, chemical activation, isotherm, methylene blue, porous carbon, spectroscopic analysis

Alagarasan Jagadeesh Kumar
Jimin Xie
Yuanguo Xu (corresponding author)
School of Chemistry and Chemical Engineering,
Jiangsu University,
Zhenjiang, Jiangsu, 212013,
China
E-mail: *xuyg@ujs.edu.cn*

Eldon R. Rene
Department of Environmental Engineering and Water Technology,
UNESCO-IHE, Institute for Water Education,
Delft 2601DA,
The Netherlands

Rajendra Prasad Singh
Department of Municipal Engineering,
Southeast University,
Nanjing, Jiangsu 210096,
China

Shasikala Siddharthy
Department of Electronics and Instrumentation,
Bharathiar University,
Coimbatore 641 046, Tamilnadu,
India

Alagarasan Jagadeesh Kumar
Chinnaiya Namasivayam
Department of Environmental Sciences,
Bharathiar University,
Coimbatore 641 046, Tamilnadu,
India

INTRODUCTION

The discharge of dye containing effluents from the textile, leather, paper and plastic industries into the environment poses severe problems to many forms of life. Methylene blue (MB) is the most commonly used chemical substance for dying cotton, wood and silk. Although MB is not strongly hazardous, it can cause some harmful effects. Acute exposure to MB can cause increased heart rate, vomiting, shock, Heinz body formation, cyanosis, jaundice, quadriplegia and tissue necrosis in humans (Theydan & Ahmed 2012). Therefore, the removal of such dyes from processed effluents becomes environmentally important.

The discharge of dyes to the environment is a matter of concern for both toxicological and aesthetic reasons, causing serious water pollution-related problems to aquatic life, e.g., reduced light penetration in water bodies. The presence of even very small amounts of dyes in water, i.e., less than 1 mg L^{-1} for some dyes, is highly visible and undesirable (Robinson *et al.* 2001; Rafatullah *et al.* 2010). There are many techniques for removing dyes from wastewater, such

doi: 10.2166/aqua.2020.132

as adsorption, coagulation, filtration, oxidation, sedimentation, precipitation and reverse osmosis (Kumar & Namasivayam 2014).

Adsorption is an efficient and economically feasible process for removing dyes from wastewater using various adsorbents (Kavitha & Namasivayam 2007a, 2007b). Activated carbon is one of the most commonly used adsorbents for dye removal due to its high surface area and large adsorption capacity (Kumar *et al.* 2017a, 2017b). A number of non-conventional adsorbents have been tested at the lab-scale for the treatment of dye-containing wastewaters. Waste materials from processing industry and agriculture are usually easily available and therefore they are considered as alternative adsorbents (Gupta & Suhas 2009). Such an approach not only converts the waste into a useful material, but it also prevents on-site burning of the waste and saves transportation and disposal costs.

Jatropha curcas is a shrub of significant economic importance due to its several potential industrial and medicinal applications (Herrera *et al.* 2006). It is a drought-resistant perennial species that grows well in marginal poor soil. Bio-diesel is made from its seeds, generating a large volume of Jatropha husk (JH). Widespread cultivation of *J. curcas* has been initiated globally. According to the Planning Commission of India, the estimated potential area of *J. curcas* plantations is 17.4 million hectares and the projected JH production is 350 million tons. As JH is rich in lignin, it has the potential to act as a good precursor for the production of activated carbon (AC), which forms the basis of any adsorbent-related research (Ramakrishnan & Namasivayam 2011).

Waste biomass has appeared in several previous studies for the removal of MB using activated carbons prepared by different activators such as periwinkle shells by KOH (Olugbenga *et al.* 2008), *Arundo donax* (Osman 2019), cork and paper waste-based (Novais *et al.* 2018), thermally activated coir pith carbon (Kavitha & Namasivayam 2007a, 2007b), cotton waste (Tian *et al.* 2019), neem leaf powder by H_2SO_4 (Patel & Vashi 2013), rice husk by HCl (Muhammad *et al.* 2012), peanut hull (Renmin *et al.* 2005), cashew nut shells (Spagnoli *et al.* 2017), $ZnCl_2$ activated *Buriti* shells (Pezoti *et al.* 2014) and activated JH husk $ZnCl_2$ (Kumar *et al.* 2017a, 2017b). Since $ZnCl_2$ is a dehydrating agent, the formation of tar during the activation of the precursor can be avoided (Caturla *et al.* 1991).

In the present study, a novel JH carbon-based adsorbent was investigated for its efficiency to remove MB from contaminated water. Batch adsorption experiments were carried out using $ZnCl_2$ activated Jatropha husk carbon (ZAJHC) and the experimental parameters, namely, pH, contact time, adsorbent dose were optimized. Isotherm, desorption and thermodynamic studies were also conducted in order to ascertain the kinetics and mechanism of the adsorption process and the reusability of the adsorbent.

MATERIALS AND METHODS

Chemical activation of Jatropha husk with zinc chloride

The washed, dried and crushed JH (450 g) was mixed with 2.0 L of warm water containing 450 g of $ZnCl_2$ for 1 h. The solution was drained and $ZnCl_2$ soaked JH was oven dried at 60 °C for 12 h. The material was filled into a steel container and fitted with a tight lid. This container was placed in another concentric steel container with another lid. The inner void space was filled with sand layers up to the brim of the container. This arrangement prevented exposure of the carbonizing material to air, allowing only a limited presence of oxygen trapped in the voids of the material being activated. The activation setup was placed in a muffle furnace for 1 h at 800 °C. After cooling, the carbon was taken out and the excess $ZnCl_2$ was leached out by immersing it in a hot 1.0 M HCl solution for 24 h and thereafter placed in a hot air oven at 80 °C. It was then repeatedly washed with hot water until the chloride content was completely removed from the wash water (tested by the silver nitrate method). This material was subsequently oven dried at 105 ± 5 °C for 8 h and sieved to 250–500 μm size (60–35 mesh ASTM) and designated as $ZnCl_2$ activated JH carbon (ZAJHC) and stored in airtight plastic containers. All the chemicals used in this study were of analytical grade (AR) and they were obtained from Loba Chemie, Mumbai.

Preparation of methylene blue solution

Figure 1 shows the molecular structure of MB. It has a molecular formula $C_{16}H_{18}ClN_3S$ with a molecular weight of 319.85. It is water soluble and blue in colour (λ_{max}, 665 nm). A stock solution of MB was prepared by dissolving an appropriate quantity of MB in distilled water. The stock solution was diluted with distilled water to obtain the desired initial MB concentrations used for the experiments.

Experimental procedures

Adsorption experiments were carried out using 25 mg of ZAJHC with 50 mL of dye solution, with the desired initial concentration and pH, at 200 rpm and 35 °C in a thermostat controlled orbital shaker (ORBITEK, Chennai, India). The MB concentration was determined spectrophotometrically by measuring the absorbance at 665 nm using an UV-Vis spectrophotometer (Specord 200, Analytic Jena, Germany). The pH was measured using a pH meter (Elico, model LI-127, Hyderabad, India).

The effect of adsorbent dosage was tested by varying the dose from 25 to 200 mg per 50 mL of dye solution, and experiments were carried out until the adsorption reached equilibrium conditions. The effect of pH was envisaged by performing experiments in the pH range of 2.0–11.0. Adsorption experiments were carried out by equilibrating (shaking, stirring) an adsorptive solution of a known composition and volume, with a known amount of adsorbent, at a constant temperature and pressure for a limited period of time. Under such conditions, it was expected that adsorption would reach a steady state or the adsorption rate would no longer change after a period of time. The adsorption of MB reached equilibrium at 120 min for a concentration of 100 mg L^{-1}, 140 min for 120 mg L^{-1} and 160 min, respectively, for other MB concentrations tested in this study. The MB removal decreased with increasing initial concentrations; however, the actual amount of dye adsorbed per unit mass of carbon increased with an increase in the MB concentration.

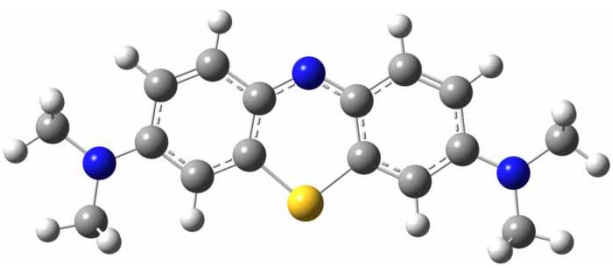

Figure 1 | Structure of methylene blue ($C_{16}H_{18}ClN_3S$).

The Langmuir, Freundlich and Dubinin–Radushkevich (D-R) isotherms were employed to study the equilibrium adsorption capacity of ZAJHC. Desorption studies were carried out at an initial dye concentration of 100 mg L^{-1}. The dye solution was separated from the adsorbent by centrifugation at 2,500 rpm for 30 min and its absorbance was measured. The dye-loaded adsorbent was filtered using Whatman filter paper and washed gently with water to remove any unabsorbed dye. Thereafter, the spent adsorbent was agitated for 120 min with 50 mL of distilled water and adjusted to different pH values. For estimating the temperature effects, the adsorption of 100 mg L^{-1} of MB by 25 mg/50 mL of adsorbent was tested at temperatures of 35, 40, 50 and 60 °C in a thermostat controlled orbital shaker (ORBITEK, Chennai, India).

Characterization of ZAJHC

The surface and structural morphologies of the loaded and unloaded ZAJHC were characterized by different analytical techniques. X-ray diffraction (XRD) was performed at room temperature using a PAN analytical X-Pert-Pro diffractometer, Westborough, USA. Infrared spectrum of the samples was obtained by using a Fourier transform infrared (FTIR) spectrometer (Bruker Tensor 27, Germany). Raman scattering was performed on a JY-1058 Raman spectrometer using a 520 nm laser source. The morphology and elemental analysis of the loaded and unloaded ZAJHC were examined using a scanning electron microscope (SEM-JSM, 840A, JEOL, Japan). The carbon samples were filtered using a suction pump on qualitative filter paper and stored in a vacuum desiccator, which was later used for instrumental analysis.

RESULTS AND DISCUSSION

Structural and morphological analysis

X-ray analysis

The XRD pattern was used to analyse the crystallinity and phases of the as-prepared ZAJHC from Jatropha husk (JH) activated by $ZnCl_2$ and the MB adsorbed ZAJHC. Figure 2(a) shows broad peaks at 23.5° and 43°, which correspond to the (002) and (100) planes, respectively. Thus, the results confirm that the ZAJHC was amorphous in structure (Bharath *et al.* 2014; Rajesh *et al.* 2014). The XRD pattern of MB adsorbed ZAJHC shows that the intensity of the (002) and (100) planes are slightly suppressed (Figure 2(a)). Borah *et al.* (2015) reported that the amorphous nature of the entire studied porous carbon (diffused peak was observed at $2\theta = 25.4°$) corresponded to the (002) diffractions of graphitic carbon. The decreased intensity of the planes may be due to the adsorbed MB on the surface and pores of the ZAJHC.

FTIR analysis

The FTIR spectra of the MB adsorbed ZAJHC are shown in Figure 2(b). As seen from this figure, the broad band at 3,420 cm^{-1} can be assigned to the stretching vibrations of hydroxyl groups -OH. The FTIR spectrum of the activated carbon shows weak and broad peaks in the region of 500–4,000 cm^{-1}. The characteristic peaks obtained at 2,926 and 2,850 cm^{-1} indicate the presence of C-H groups. The MB loaded ZAJHC shows a peak at 1,574 cm^{-1} which was shifted to 1,570 cm^{-1} and can be attributed to the N-H vibration coupled with the C-N stretching mode, indicating the saturation of the material with MB (Lua & Yang 2005; Heidarinejad *et al.* 2018; Jamshaid *et al.* 2019). The band at 1,065 cm^{-1} can be assigned to esters (Pezoti *et al.* 2014). The main change observed after adsorption of

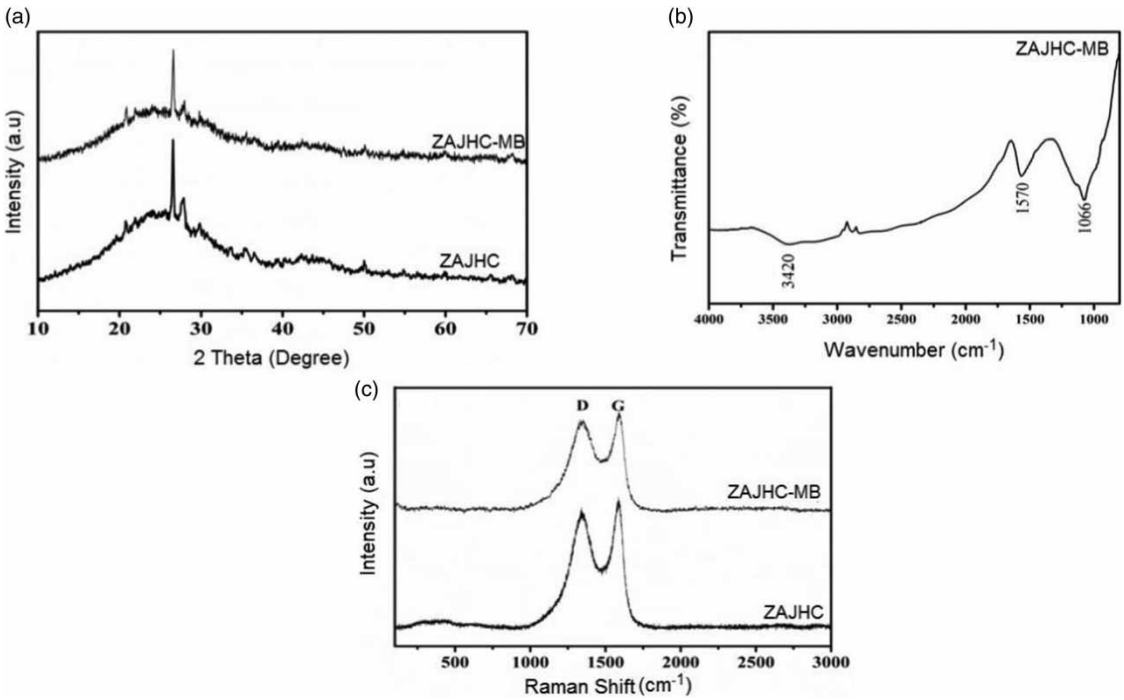

Figure 2 | (a) X-ray diffraction patterns of ZAJHC and ZAJHC after adsorption of MB, (b) FTIR spectra of ZAJHC-MB and (c) Raman spectra of ZAJHC and ZAJHC after the adsorption of MB.

the dye molecule was splitting of the strong stretching of C = O into small splits (Figure 2(b)).

Raman analysis

Raman spectra (Figure 2(c)) provide structural analysis of ZAJHC and MB adsorbed ZAJHC. ZAJHC shows two prominent peaks at 1,340 and 1,585 cm^{-1} which correspond to the well documented D and G bands, respectively. The weak D band at 1,340 cm^{-1} is associated with the vibration of A_{1g} symmetry of sp^3 carbon atoms and associated with defect ordered structural peak. The peak G relates to the first-order scattering of the E_{2g} phonon of carbon sp^2 atoms and second-order double resonant process with opposite momentum in the highest optical branch near the K points in the Brillouin zone (Bz) of the carbon atom. The D and G band ratio of ZAJHC (I_{1340}/I_{1585}) was 0.7, which indicates a unique amorphous carbon structure and a high content of lattice edges or plane defects of ZAJHC (Bharath *et al.* 2014; Rajesh *et al.* 2014). The intensity ratio (I_D/I_G) of the MB adsorbed ZAJHC was 0.96, which indicates that the defects increased due to the adsorption of MB on the surface of ZAJHC (Figure 2(c)).

Morphological analysis

The morphology of the ZAJHC and MB loaded ZAJHC was observed through SEM micrographs. Figure 3(a) and 3(b)

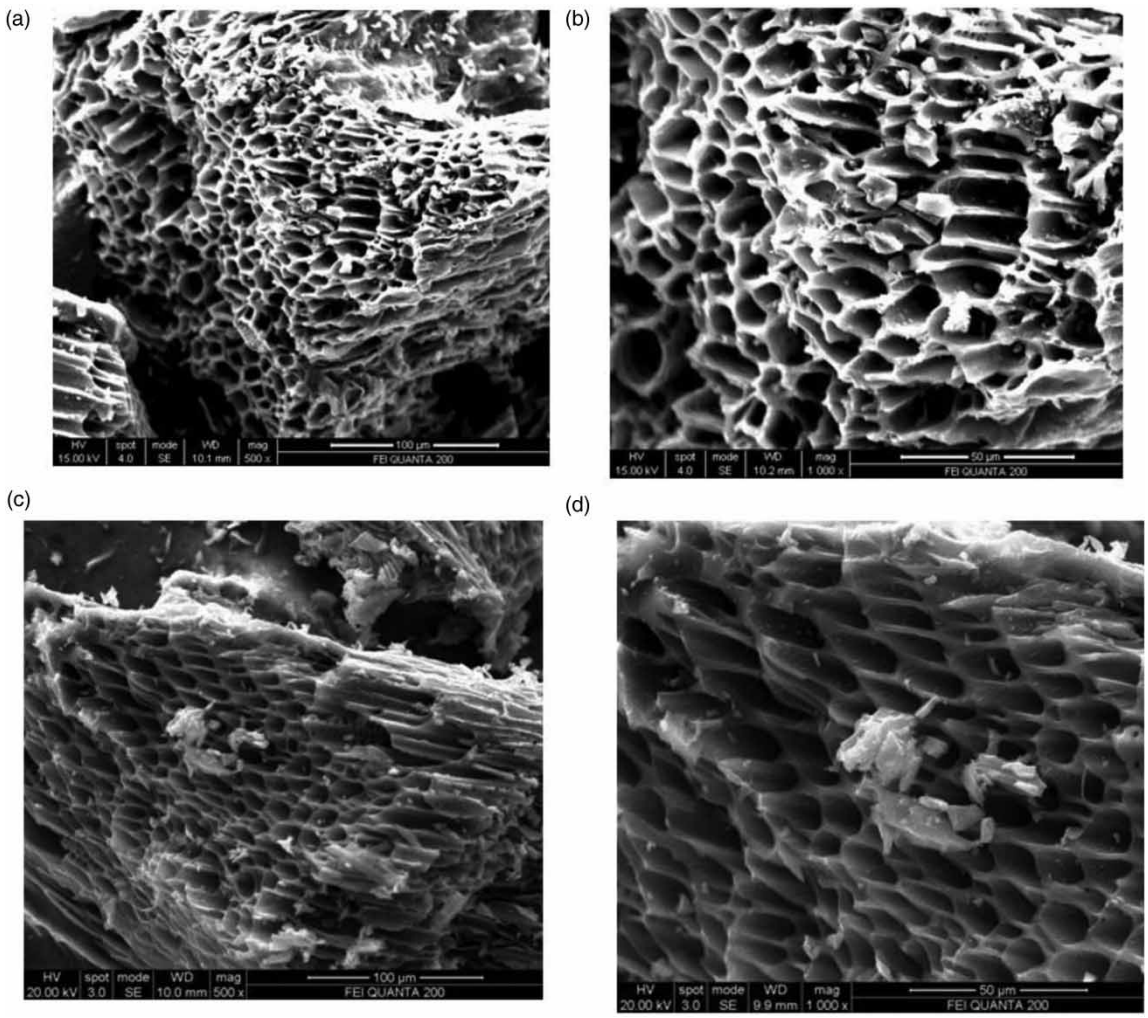

Figure 3 | SEM images with different magnification images of (a) and (b) ZAJHC and (c) and (d) ZAJHC after the adsorption of MB.

show tremendous, perfect and constructed pore structures on the surface of ZAJHC. In this study, the carbon was compressed and the appearance of the lanky structure is due to the formation of more interspaces between the monolayers of the carbon, presumably due to activation using $ZnCl_2$. A higher volume of pores developed from the $ZnCl_2$ activation acts as a route for the contaminants to enter into the micropores (Ramakrishnan & Namasivayam 2011). Basically, the high SSA and pore structure are the basic parameters for an effective adsorbent. When the porosity of the JHC and ZAJHC increases, the SSA also increases (Mohanty *et al.* 2005; Borah *et al.* 2015). After adsorption, the surface turned into a more irregular structure (Kumar *et al.* 2017a, 2017b). Evidently, the dye molecules were strongly adsorbed onto the surface of ZAJHC (Figure 3(c) and 3(d)).

Adsorption kinetics and mechanism

Effect of pH

The effect of pH on the removal of MB is shown in Figure 4(a). The per cent removal was >85% in the pH range of 2.0–11.0. At pH 10.0, negatively charged surface sites on the adsorbent will favour the adsorption of dye cations due to the electrostatic attraction and hence dye removal was high (i.e., >85%). In this study, although the pH was decreased, the removal of MB was still ~70%. Basically, MB and other cationic dyes produce an intense molecular cation (C^+) and reduced ions (CH^+). At high pH, OH^- on the surface of adsorbent will favour the adsorption of cationic dye molecules. Many previous works have also reported that MB adsorption efficiency onto carbon-based adsorbents usually increases as the pH is increased (Kavitha & Namasivayam 2007a, 2007b).

Desorption studies

Desorption studies were conducted as a function of pH in order to analyse the possibility of reusing the adsorbent for many adsorption cycles and to make the process more economical. At lower pH, the hydrogen ion (H^+) concentration increases in solution, which then displaces the adsorbed dye cations into solution. In this study, the desorption efficiency decreased from 35.2% at pH 2.0 to 19.5% at pH 10.0, at an MB concentration of 100 mg L^{-1} (Figure 4(b)) (Chen *et al.* 2013). The reversibility of the adsorbed dyes is in agreement with the pH-dependent results obtained. The better desorption efficiency of dye molecules at low pH indicates that adsorption of MB on to ZAJHC may be due to the mechanism of ion-exchange (Ofomaja & Ho 2008).

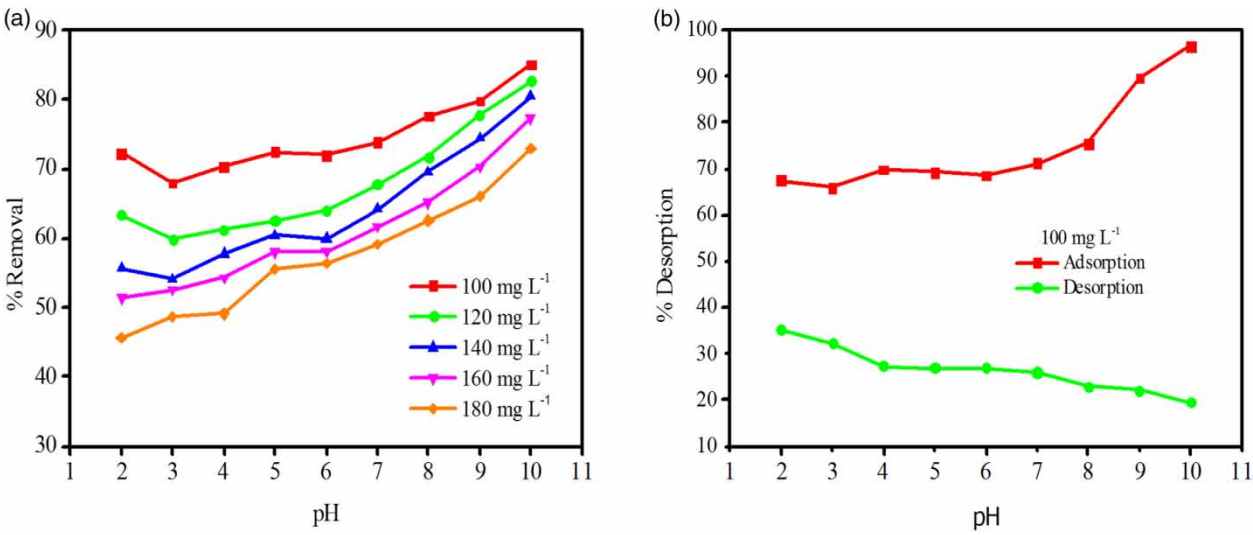

Figure 4 | Effect of pH on the (a) adsorption of MB by ZAJHC and (b) desorption of MB from ZAJHC.

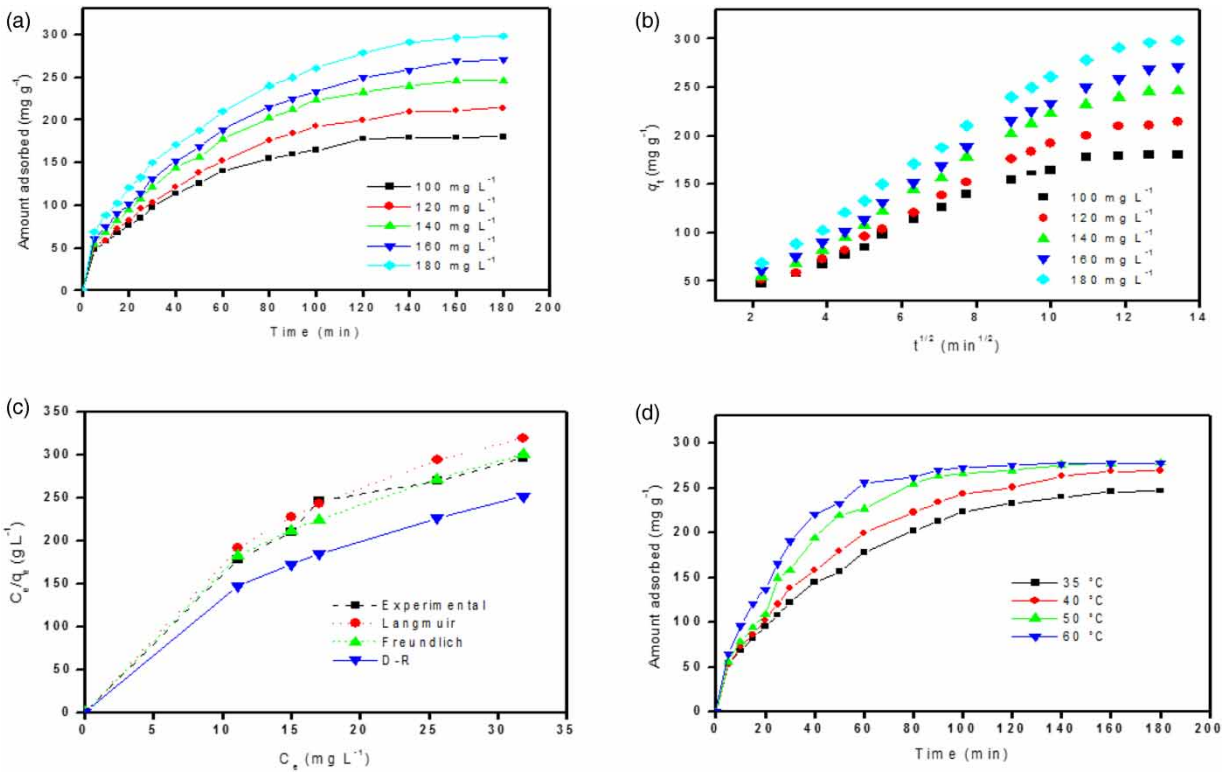

Figure 5 | (a) Effect of agitation time and initial MB concentration on the amount of MB adsorbed by ZAJHC, (b) intraparticle diffusion plots for the adsorption of MB by ZAJHC, (c) comparison of Langmuir, Freundlich and D-R isotherms for the adsorption of MB by ZAJHC and (d) effect of temperature on the adsorption of MB by ZAJHC.

Effect of contact time

In order to study the effect of contact time, the initial MB concentrations were varied from 100 to 180 mg L^{-1} at 35 °C (Figure 5(a)). The adsorption of MB reached equilibrium at 120 min for 100 mg L^{-1}, 140 min for 120 mg L^{-1} and 160 min for other MB concentrations. The MB removal decreased with increasing initial concentrations, but the actual amount of dye adsorbed per unit mass of carbon increased with an increase in the MB concentration. This implies that the adsorption is highly dependent on the initial concentration of dye. At lower concentration, however, the ratio of the initial number of dye molecules to the available surface area is low. The MB uptake profiles, as a function of time, show a smooth and continuous curve that leads to saturation which suggests the possibility of monolayer coverage of dye on the surface of the adsorbent (Borah *et al.* 2015). On the other hand, at high MB concentrations, the available sites of adsorption become fewer and hence the removal of MB is dependent upon the initial concentration (Malik 2003). The ZAPHC S_{BET} ($m^2 g^{-1}$) 822 is mentioned in Table 1.

Adsorption kinetics

Table 2 shows the values of k_1, which were calculated from the slopes of the linear plots derived from the computed results obtained from the first- and second-order kinetic

Table 1 | Physico-chemical characteristics of ZAJHC (Kumar *et al.* 2017a, 2017b)

Parameter	Value
pH_{zpc}	6.8
Specific gravity	1.03
Bulk density (g L^{-1})	0.20
Porosity (%)	81
S_{BET} ($m^2 g^{-1}$)	822
Ion exchange capacity (meq g^{-1})	Nil
Iodine number (mg g^{-1})	91

Table 2 | Kinetic parameters for the adsorption of MB onto ZAJHC

Kinetic model	Conc. (mg L^{-1})	q_e exp (mg g^{-1})	k_1 (min^{-1})	q_e cal (mg g^{-1})	R^2
First-order	100	177.75	0.023	161.06	0.995
	120	209.99	0.023	207.01	0.985
	140	245.95	0.023	255.85	0.982
	160	269.01	0.0207	263.02	0.984
	180	296.31	0.023	311.17	0.945
	Conc. (mg L^{-1})	q_e exp (mg g^{-1})	k_2 (g mg^{-1} min^{-1})	q_e cal (mg g^{-1})	R^2
Second-order	100	177.75	0.00011	250	0.973
	120	209.99	6.2×10^{-5}	333.3	0.968
	140	245.95	6.9×10^{-5}	357.1	0.979
	160	269.01	7.4×10^{-5}	416.6	0.976
	180	296.31	3.9×10^{-5}	500	0.978
	Conc. (mg L^{-1})	q_e exp (mg g^{-1})	k_{id} (mg g^{-1} $h^{-1/2}$)	C	R^2
	100	177.75	13.23	34.38	0.941
	120	209.99	16.52	27.15	0.962
	140	245.95	19.11	31.34	0.96
	160	269.01	20.78	31.76	0.972
Intraparticle diffusion	180	296.31	22.36	42.56	0.972

models along with the experimental determined q_e values which are also shown in Table 2. k_1 and k_2 are the rate constants for pseudo first-order and second-order equations, respectively. Table 2 shows the kinetic data parameters which revealed that MB for pseudo first-order was higher than that of second-order. This implies that the adsorption of MB by ZAJHC adsorbent could be represented by the pseudo first-order kinetic model. In addition, the theoretical q_e cal values for pseudo first-order model were found to be closer to the experimental (q_e exp) values. This result is also in agreement with previously reported literature (Martins *et al.* 2006).

Intraparticle diffusion plot

According to the results shown in Figure 5(b), the initial curved portion can be attributed to the bulk diffusion effect, the linear portion to the intraparticle diffusion effect and the plateau to the equilibrium condition. The plots of q_t vs k_{id} have the same general features as shown in Figure 5(b). The linear portions of the plots do not pass through the origin indicating that intraparticle diffusion is not the only rate controlling step for the adsorption process. The slopes of the linear portions of the plots of q_t vs $t^{1/2}$ give the values of k_{id} (Table 2). The values of the intercept provide information about the thickness of the boundary layer, i.e., the larger the intercept, the greater the boundary layer effect (Kannan & Sundaram 2001). The linear portions of this plot can be attributed to the instantaneous utilization of the most readily available adsorbing sites on the adsorbent surface.

Adsorption isotherms

The Langmuir constants Q_0 and b were found to be 500 mg g^{-1} and 0.056 (L mg^{-1}), respectively. The essential characteristics of the Langmuir isotherm can be expressed by a dimensionless constant called the equilibrium parameter R_L. The R_L values were found to vary between 0 and 1 which indicates a favourable adsorption process (Table 3). The Freundlich constants, k_f and n were calculated from the linear plot of log q_e vs log C_e (Table 3). Table 4 compares the Langmuir, Freundlich and D-R constants for adsorption of MB onto various adsorbents as reported in the literature. The Freundlich model assumes heterogeneous adsorption due to the diversity of sorption sites or the diverse nature of the adsorbate adsorbed, free or hydrolyzed species. On the other hand, the adsorption capacity based on the D-R isotherm is independent of the operating temperature, but it varies depending on the nature of adsorbent and the adsorbate.

Table 3 | Langmuir, Freundlich and Dubinin–Radushkevich isotherm constants for the adsorption of MB onto ZAJHC

		Langmuir					Freundlich				D-R			
Dye	Conc. mg L^{-1}	Q_o (mg g^{-1})	b (L mg^{-1})	R^2	R_L	Δq (%)	k_f ($mg^{1-1/n}$ $L^{1/n}$ g^{-1})	n	R^2	Δq (%)	q_m (mg g^{-1})	β (mol^2 $J^2 \times 10^{-9}$)	R^2	Δq (%)
MB	100				0.15									
	120				0.13									
	140	500	0.056	0.977	0.11	8.21	59.84	2.14	0.94	4.64	2,334	4	0.945	20.81
	160				0.10									
	180				0.09									

Table 4 | Comparison of literature reports on Langmuir, Freundlich and D-R constants for the adsorption of MB onto various adsorbents

	Langmuir isotherm		Freundlich isotherm		D-R isotherm	
Adsorbent	Q_o (mg g^{-1})	b (mg L^{-1})	k_f ($mg^{1-1/n}$ $L^{1/n}$ g^{-1})	n	E (kJ mol^{-1})	Reference
ZAJHC	500	0.056	68.34	2.14	11.18	This study
Neem leaf powder (NLP)	402	*	4.99	1.43	*	Patel & Vashi (2013)
Activated NLP	353	*	4.84	1.46	*	Patel & Vashi (2013)
Activated carbon (rice husk-H_3PO_4 impregnated)	333.3	0.043	57.54	2.86	*	Singh & Srivastava (2001)
Carbon slurry waste	96.2	6.67×10^4	*	*	*	Jain *et al.* (2003)
Coir pith carbon	5.87	0.93	1.192	0.705	3.54	Kavitha & Namasivayam (2007a, 2007b)
Date press cake	546	*	*	*	*	Heidarinejad *et al.* (2018)

* refers to not reported.

The mean free energy of adsorption gives information about the chemical ion-exchange mechanism. The E value varied between 8 and 16 kJ mol^{-1} and thus the adsorption process follows the ion-exchange mechanism. On the other hand, if $E < 8$ kJ mol^{-1}, the adsorption process is physical in nature. The mean energy of the MB adsorption was calculated as 11.18 kJ mol^{-1}, which indicates that the adsorption of MB on the ZAJHC occurred by ion-exchange mechanism. The D-R constants of various adsorbents for MB reported in the literature are presented in Table 4. Figure 5(c) presents the different adsorption isotherms fitted to the experimental data of this study. Based on the results shown in Table 3, the Freundlich isotherm has the lowest Δq and, therefore, it is most suitable to represent the adsorption of MB onto ZAJHC than the other isotherms.

Effect of adsorbent dose, concentration and temperature

The removal of MB by ZAJHC at different adsorbent doses (25–200 mg/50 mL) and different initial concentrations of MB from 100 to 180 mg L^{-1} was studied. It was observed that an increase in the adsorbent dose increased the removal of MB and this can be attributed to the greater surface area and the availability of more adsorption sites on ZAJHC (Arivoli *et al.* 2008). An increase of temperature increased the MB removal (Figure 5(d)). The positive value of ΔH° (3.86 J mol^{-1} K^{-1}) shows the endothermic nature of the adsorption process. The negative values of ΔG° indicate the spontaneous nature of adsorption for MB. Table 5 shows positive values of ΔS° (65.86 J mol^{-1} K^{-1}) which suggest an increased randomness at the solid/solution

Table 5 | Thermodynamic parameters for the adsorption of MB onto ZAJHC

T (K)	K_c	ΔG (kJ mol^{-1})	ΔH (kJ mol^{-1})	ΔS (J mol^{-1} K^{-1})
308	7.19	−5.05		
313	23.03	−8.16		
323	69.42	−11.38	3.86	65.86
333	92.45	−12.53		

interface during the adsorption of dye by ZAJHC (Namasivayam & Sumithra 2005).

CONCLUSIONS

The pure ZAJHC and MB-adsorbed ZAJHC were characterized using XRD, FTIR and Raman spectroscopy. The prepared ZAJHC shows an excellent dye removal capacity at initial concentrations <180 mg L^{-1}. The pH of the dye solution strongly affected the chemistry of both the dye molecules and the adsorbent in aqueous solutions. The adsorption process was governed by the mechanism of ion-exchange and it followed Lagergren's first-order kinetics.

ACKNOWLEDGEMENTS

This research was supported by the National Natural Science foundation of China (Grant No. 51650410657). ERR thanks IHE-Delft (The Netherlands) for providing staff time support to collaborate with researchers from China.

REFERENCES

Arivoli, S., Hema, M., Karuppaiah, M. & Saravanan, S. 2008 Adsorption of chromium ion by acid activated low cost activated carbon-kinetic, mechanistic, thermodynamic and equilibrium studies. *E-J. Chem.* **5** (4), 820–831.

Bharath, G., Jagadeesh, K. A., Karthick, K., Mangalaraj, D., Viswanathan, C. & Ponpandian, N. 2014 Shape evolution and size controlled synthesis of mesoporous hydroxyapatite nanostructures and their morphology dependent Pb(II) removal from waste water. *RSC Adv.* **4**, 37446.

Borah, L., Goswami, M. & Phukan, P. 2015 Adsorption of methylene blue and eosin yellow using porous carbon prepared from tea waste: adsorption equilibrium, kinetics and thermodynamics study. *J. Environ. Chem. Eng.* **3**, 1018–1028.

Caturla, F., Molina-Sabio, M. & Reinoso, F. R. 1991 Preparation of activated carbon by chemical activation with $ZnCl_2$. *Carbon* **29**, 999–1007.

Chen, M., Ding, W., Wang, J. & Diao, G. 2013 Removal of azo dyes from water by combined techniques of adsorption, desorption, and electrolysis based on a supramolecular sorbent. *Ind. Eng. Chem. Res.* **52**, 2403–2411.

Gupta, V. K. & Suhas. 2009 Application of low-cost adsorbents for dye removal – a review. *J. Environ. Manage.* **90**, 2313–2342.

Heidarinejad, Z., Rahmanian, O., Fazlzadeh, M. & Heidari, M. 2018 Enhancement of methylene blue adsorption onto activated carbon prepared from date press cake by low frequency ultrasound. *J. Mol. Liq.* **264** (15), 591–599.

Herrera, M. J., Siddhuraju, P., Francis, G., Davila-Ortiz, G. & Becker, K. 2006 Chemical composition, toxic/antimetabolic constituents, and effects of different treatments on their levels, in four provenances of *Jatropha curcas* L. from Mexico. *Food Chem.* **96**, 80–89.

Jain, A. K., Gupta, V. K., Bhatngar, A., Jain, S. & Suhas, A. I. 2003 A comparative assessment of adsorbents prepared from industrial wastes for the removal of cationic dye. *J. Ind. Chem. Soc.* **80**, 267–270.

Jamshaid, R., Fakhra, T., Adeela, R. & Rajeev, K. 2019 Synthesis using natural functionalization of activated carbon from pumpkin peels for decolourization of aqueous methylene blue. *Sci. Total Environ.* **671**, 369–376.

Kannan, K. & Sundaram, M. M. 2001 Kinetics and mechanism of removal of methylene blue by adsorption on various carbons – a comparative study. *Dyes Pigm.* **51**, 25–40.

Kavitha, D. & Namasivayam, C. 2007a Experimental and kinetic studies on methylene blue adsorption by coir pith carbon. *Biores. Technol.* **98**, 14–21.

Kavitha, D. & Namasivayam, C. 2007b Recycling coir pith, an agricultural solid waste, for the removal of procion orange from wastewater. *Dyes Pigm.* **74**, 237–248.

Kumar, A. J. & Namasivayam, C. 2014 Uptake of endocrine disruptor bisphenol-A onto sulphuric acid activated carbon developed from biomass: equilibrium and kinetic studies. *Sustain. Environ. Res.* **24** (1), 73–80.

Kumar, A. J., Rajendra, P. S., Dafang, F. & Chinnaiya, N. 2017a Low cost meso-porous carbon developed from Jatropha husk, a bio-diesel by-product waste for adsorption of methylene blue. *Fresen. Environ. Bull.* **26** (10), 5723–5731.

Kumar, A. J., Rajendra, P. S., Fu, D. & Chinnaiya, N. 2017b Comparison of physical- and chemical-activated *Jatropha curcas* husk carbon as an adsorbent for the adsorption of Reactive Red 2 from aqueous solution. *Desalin. Water Treat.* **95**, 308–318.

Lua, A. C. & Yang, T. 2005 Characteristics of activated carbon prepared from pistachio-nut shell by zinc chloride activation under nitrogen and vacuum conditions. *J. Colloid Interface Sci.* **290**, 505–513.

Malik, P. K. 2003 Use of activated carbons prepared from sawdust and rice-husk for adsorption of acid dyes: a case study of Acid Yellow 36. *Dyes Pigm.* **56** (3), 239–249.

Martins, B. L., Cruz, C. C. V., Luna, A. S. & Henriques, C. A. 2006 Sorption and desorption of Pb^{2+} ions by dead *Sargassum* sp. Biomass. *Biochem. Eng. J.* **27**, 310–314.

Mohanty, K., Jha, M., Meikap, B. C. & Biswas, M. N. 2005 Removal of chromium(VI) from dilute aqueous solutions by activated carbon developed from *Terminalia arjuna* nuts activated with zinc chloride. *Chem. Eng. Sci.* **60** (11), 3049–3059.

Muhammad, N. A., Muhammad, N. U. H., Tahira, A., Ambreen, S., Ashfaq, M. & Muhammad, N. 2012 Methylene blue adsorption onto granular activated carbon prepared from harmal seeds residue. *Desalin. Water Treat.* **49**, 376–383.

Namasivayam, C. & Sumithra, S. 2005 Removal of direct red 12B and methylene blue from water by adsorption onto Fe (III)/Cr (III) hydroxide, an industrial solid waste. *J. Environ. Manage.* **74**, 207–221.

Novais, R. M., Caetano, A. P. F., Seabra, M. P., Labrincha, J. A. & Pullar, R. C. 2018 Extremely fast and efficient methylene blue adsorption using eco-friendly cork and paper waste-based activated carbon adsorbents. *J. Clean Prod.* **197**, 1137–1147.

Ofomaja, E. & Ho, Y. S. 2008 Effect of temperatures and pH on methyl violet bio sorption by *mansonia* wood sawdust. *Bioresour. Technol.* **99**, 5411–5417.

Olugbenga, S. B., Idowu, A. A., John, C. A. & Ezekiel, O. F. 2008 Adsorption of methylene blue onto activated carbon derived from periwinkle shells: kinetics and equilibrium studies. *Chem. Ecol.* **24** (4), 285–295.

Osman, U. 2019 Hydrogen storage capacity and methylene blue adsorption performance of activated carbon produced from Arundo donax. *Mater. Chem. Phys.* **237**, 121858.

Patel, H. & Vashi, R. T. 2013 A comparison study of removal of methylene blue dye by adsorption on neem leaf powder (NLP) and activated NLP. *J. Environ. Eng. Lands. Manage.* **21** (1), 36–41.

Pezoti, J. O., Cazetta, A. L., Souza, I. P. A. F., Bedin, K. C., Martins, A. C., Silva, T. L. & Almeida, V. 2014 Adsorption studies of methylene blue onto zncl$_2$-activated carbon produced from buriti shells *Mauritia flexuosa L. J. Ind. Eng. Chem.* **20** (6), 4401–4407.

Rafatullah, M., Sulaiman, O., Hashim, R. & Ahmad, A. 2010 Adsorption of methylene blue on low-cost adsorbents: a review. *J. Hazard. Mater.* **177**, 70–80.

Rajesh, M., Veeramani, V. & Shen, M. C. 2014 Heteroatom-enriched and renewable banana-stem-derived porous carbon for the electrochemical determination of nitrite in various water samples. *Sci. Rep.* **4**, 4679.

Ramakrishnan, K. & Namasivayam, C. 2011 Zinc chloride-activated jatropha husk carbon for removal of phenol from water by adsorption: equilibrium and kinetic studies. *Toxicol. Environ. Chem.* **93** (6), 1111–1122.

Renmin, G., Yingzhi, S., Jianb, C., Huijun, L. & Chao, Y. 2005 Effect of chemical modification on dye adsorption capacity of peanut hull. *Dyes Pigm.* **67**, 175–181.

Robinson, T., McMullan, G., Marchant, R. & Nigam, P. 2001 Remediation of dyes in textiles effluent: a critical review on current treatment technologies with a proposed alternative. *Bioresour. Technol.* **77**, 247–255.

Singh, D. K. & Srivastava, B. 2001 Basic dyes removal from waste water by adsorption on rice husk carbon. *Ind. J. Chem. Technol.* **8**, 133–139.

Spagnoli, A. A., Giannakoudakis, D. A. & Bashkova, S. 2017 Adsorption of methylene blue on cashew nut shell based carbons activated with zinc chloride: the role of surface and structural parameters. *J. Mol. Liq.* **229**, 465–471.

Theydan, S. K. & Ahmed, M. J. 2012 Adsorption of methylene blue onto biomass-based activated carbon by $FeCl_3$ activation: equilibrium, kinetics, and thermodynamic studies. *J. Anal. Appl. Pyrolysis* **97**, 116–122.

Tian, D., Xu, Z., Zhang, D., Chen, W., Cai, J., Deng, H., Sun, Z. & Zhou, Y. 2019 Micro mesoporous carbon from cotton waste activated by $FeCl_3/ZnCl_2$: preparation, optimization, characterization and adsorption of methylene blue and eriochrome black T. *J. Solid State Chem.* **269**, 580–587.

First received 17 August 2019; accepted in revised form 3 February 2020. Available online 6 April 2020